A Modified Optimal Control Strategy for a Five-Finger Robotic Hand

Cheng-Hung Chen[1,2,*] and D. Subbaram Naidu[3]

[1]*Department of Mechanical and Industrial Engineering, University of Massachusetts, 160 Governors Drive, Amherst, MA 01003, USA*

[2]*Institut für Astronomische und Physikalische Geodäsie, Technische Universität München, Arcisstraße 21, 80333 München, Germany*

[3]*Minnesota Power Jack Rowe Endowed Chair for Energy and Controls and Professor of Electrical Engineering, University of Minnesota at Duluth, 273 MWAH, 1023 University Drive, Duluth, MN 55812, USA*

Abstract: This paper addresses a modified optimal control strategy for a 14-degrees-of-freedom, five-finger robotic hand to improve accuracy and reduce convergence time by modifying the performance index embedded with an exponential term. First, the trajectory planning of the joints of each finger is designed by using cubic polynomial. Then the kinematic and dynamic equations of the robotic hand and feedback linearization technique are employed. Next, the original and modified optimal control methods are applied to the robotic hand. Finally, simulations show that the proposed modified optimal control technique provides much faster response with high accuracy compared to a hybrid genetic algorithm-tuned PID control.

Keywords: Robotic Hand, Optimal Control, Hybrid Control, PID Control, Genetic Algorithm, Prosthetic Hand.

I. INTRODUCTION

Our previous works showed that proportional-integral-derivative (PID) control with genetic algorithm (GA) tuning parameters increases convergence speed for a five-finger robotic hand [1, 2], but the GA-PID controller causes undesirable characteristic of overshooting and oscillation, which was also shown in other robot applications by researchers [3, 4]. Optimal control [5] with specific applications to robotic hand devices can obtain a high performance to overcome the overshooting and oscillation problems [1, 6], but requires large convergence time. Therefore, developing a modified optimal control strategy for a 14-degrees-of-freedom (DoF), five-finger robotic hand is the main aim of this work and this control technique can be also used in other robotics applications, including hazardous environments, surgery, and clinical prosthetic hands [7-9]. Recently, we have organized control strategies for robotic devices and prosthetic hands [10, 11].

In this work, we briefly introduce feedback linearization technique and then develop an original finite-time linear quadratic optimal controller for a five-finger robotic hand. We then detail the modified finite-time linear quadratic optimal control adding an exponential term in its cost function or performance index. Simulation results demonstrate that the proposed modified optimal control technique gives fast response and high accuracy without increasing computational time compared to a hybrid GA-tuned PID control.

*Address correspondence to this author at the Department of Mechanical and Industrial Engineering, University of Massachusetts, 160 Governors Drive, Amherst, MA 01003, USA and Institut für Astronomische und Physikalische Geodäsie, Technische Universität München, Arcisstraße 21, 80333 München, Germany; Tel: +1 617-388-1509; E-mail: nthumary@gmail.com, chenchen@isu.edu

II. CONTROL STRATEGIES

A. Modeling

Human hand anatomy, trajectory planning of fingertips using cubic polynomial, kinematics (including forward, inverse and differential kinematics) and dynamics of the hand for a five-finger robotic hand have been developed in our previous studies [12, 13]. This paper uses same symbols as our previous work.

B. Feedback Linearization

We use feedback linearization technique to put nonlinear dynamics into a linear state-variable system. Alternative state-space equations of the dynamics can be obtained by defining the angular position/velocity state $\mathbf{x}(t)$ of the joints as

$$\mathbf{x}(t) = \left[\mathbf{q}'(t) \;\; \dot{\mathbf{q}}'(t)\right]'. \tag{1}$$

$\mathbf{q}'(t)$ and $\dot{\mathbf{q}}'(t)$ are the transpose vectors of angular position $\mathbf{q}(t)$ and angular velocity $\dot{\mathbf{q}}(t)$, respectively. Let us repeat the dynamical model and rewrite it as

$$\frac{d}{dt}\dot{\mathbf{q}}(t) = -\mathbf{M}^{-1}(\mathbf{q}(t))[\mathbf{N}(\mathbf{q}(t), \dot{\mathbf{q}}(t)) - \boldsymbol{\tau}(t)], \tag{2}$$

where $\mathbf{M}(\mathbf{q}(t))$ is inertia matrix and $\mathbf{N}(\mathbf{q}(t),\dot{\mathbf{q}}(t)) = \mathbf{C}(\mathbf{q}(t),\dot{\mathbf{q}}(t)) + \mathbf{G}(\mathbf{q}(t))$ represents nonlinear terms. $\mathbf{C}(\mathbf{q}(t),\dot{\mathbf{q}}(t))$ is a Coriolis/centripetal vector and $\mathbf{G}(\mathbf{q}(t))$ is a gravity vector. $\boldsymbol{\tau}(t)$ is a given torque vector at joints.

From (1) and (2), we can then derive a *linear* system in Brunovsky canonical form as

$$\dot{\mathbf{x}}(t) = \begin{bmatrix} \mathbf{0} & \mathbf{I} \\ \mathbf{0} & \mathbf{0} \end{bmatrix}\mathbf{x}(t) + \begin{bmatrix} \mathbf{0} \\ \mathbf{I} \end{bmatrix}\mathbf{u}(t) = \mathbf{A}\mathbf{x}(t) + \mathbf{B}\mathbf{u}(t) \tag{3}$$

with its control input vector given by

$$\mathbf{u}(t) = -\mathbf{M}^{-1}(\mathbf{q}(t))[\mathbf{N}(\mathbf{q}(t),\dot{\mathbf{q}}(t)) - \boldsymbol{\tau}(t)]. \tag{4}$$

The required torque of all joints can be then calculated by

$$\boldsymbol{\tau}(t) = \mathbf{M}(\mathbf{q}(t))\mathbf{u}(t) + \mathbf{N}(\mathbf{q}(t),\dot{\mathbf{q}}(t)). \tag{5}$$

C. Linear Quadratic Optimal Control with Tracking System

Our objective is to control the linear system (3) in such a way that the state variable $\mathbf{x}(t) = \left[\mathbf{q}'(t)\ \ \dot{\mathbf{q}}'(t)\right]'$ *tracks* the *desired* output $\mathbf{z}(t) = \left[\mathbf{q}_d'(t)\ \ \dot{\mathbf{q}}_d'(t)\right]'$ as close as possible during the interval $[t_0, t_f]$ with minimum control energy. For this, let us define the *error* vector as

$$\mathbf{e}(t) = \mathbf{z}(t) - \mathbf{x}(t), \tag{6}$$

and choose the performance index J [5] as

$$J = \frac{1}{2}\mathbf{e}'(t_f)\mathbf{F}(t_f)\mathbf{e}(t_f) + \frac{1}{2}\int_{t_0}^{t_f}\left[\mathbf{e}'(t)\mathbf{Q}\mathbf{e}(t) + \mathbf{u}'(t)\mathbf{R}\mathbf{u}(t)\right]dt. \tag{7}$$

We assume that $\mathbf{F}(t_f)$ and $\mathbf{Q}$ are symmetric, *positive semidefinite* matrices, and $\mathbf{R}$ is symmetric, *positive definite* matrix. We use Pontryagin Minimum Principle [5] and then solve the matrix differential Riccati equation (DRE)

$$\dot{\mathbf{P}}(t) = -\mathbf{P}(t)\mathbf{A} - \mathbf{A}'\mathbf{P}(t) + \mathbf{P}(t)\mathbf{B}\mathbf{R}^{-1}\mathbf{B}'\mathbf{P}(t) - \mathbf{Q}, \tag{8}$$

with final condition $\mathbf{P}(t_f) = \mathbf{F}(t_f)$, and the non-homogeneous vector differential equation

$$\dot{\mathbf{g}}(t) = -\left[\mathbf{A} - \mathbf{B}\mathbf{R}^{-1}\mathbf{B}'\mathbf{P}(t)\right]'\mathbf{g}(t) - \mathbf{Q}\mathbf{z}(t), \tag{9}$$

with final condition $\mathbf{g}(t_f) = \mathbf{F}(t_f)\mathbf{z}(t_f)$. Then the optimal state $\mathbf{x}^*(t)$ can be solved from

$$\dot{\mathbf{x}}^*(t) = \left[\mathbf{A} - \mathbf{B}\mathbf{R}^{-1}\mathbf{B}'\mathbf{P}(t)\right]\mathbf{x}^*(t) + \mathbf{B}\mathbf{R}^{-1}\mathbf{B}'\mathbf{g}(t) \tag{10}$$

with initial condition $\mathbf{x}(t_0)$ and optimal control $\mathbf{u}^*(t)$ is calculated by

$$\mathbf{u}^*(t) = -\mathbf{R}^{-1}\mathbf{B}'\mathbf{P}(t)\mathbf{x}^*(t) + \mathbf{R}^{-1}\mathbf{B}'\mathbf{g}(t). \tag{11}$$

Finally, the optimal required torque $\boldsymbol{\tau}^*(t)$ is obtained by

$$\boldsymbol{\tau}^*(t) = \mathbf{M}(\mathbf{q}(t))\mathbf{u}^*(t) + \mathbf{N}(\mathbf{q}(t),\dot{\mathbf{q}}(t)). \tag{12}$$

Summarizing, Figure **1** shows the block diagram of a finite-time linear quadratic optimal controller tracking system for the robotic hand. Use of feedback linearization technique converts the nonlinear dynamics to linear. Then the closed-loop finite-time linear quadratic optimal controller through Pontryagin Minimum Principle is implemented to track the desired trajectory planning using cubic polynomial. $\mathbf{P}(t)$ and $\mathbf{g}(t)$ are computed by solving the matrix differential Riccati and the non-homogeneous vector differential equations with boundary conditions, respectively.

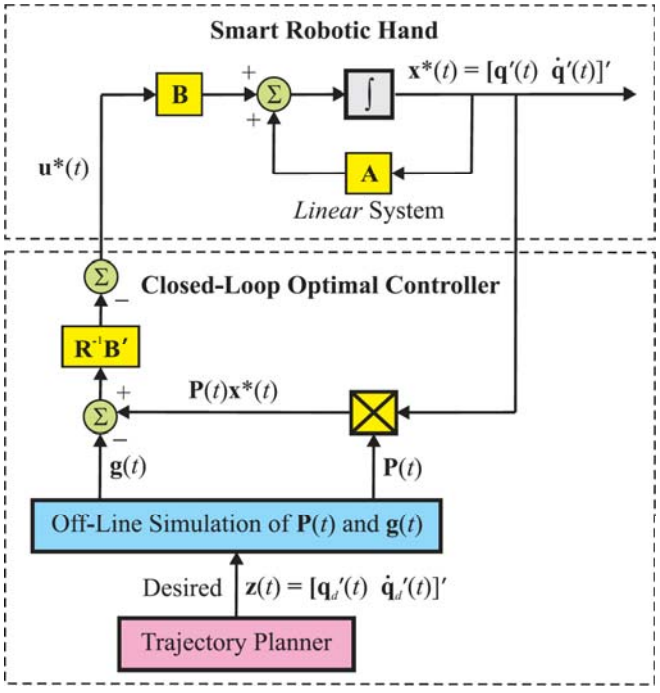

Figure 1: Block diagram of the linear quadratic optimal controller tracking system for the five-finger robotic hand.

Finally, the optimal state $\mathbf{x}^*(t)$ and optimal control $\mathbf{u}^*(t)$ are obtained in order to calculate the required torque $\boldsymbol{\tau}^*(t)$.

D. A Modified Optimal Control with Tracking System

Our previous works [1, 6] showed that the original optimal control can avoid overshooting and oscillation problems and get better results than GA-tuned PID control [1, 2], but this optimal control method takes execution time when applied to the robotic hand. To improve the performance of the original optimal controller, we change the performance index $\hat{J}$ [5] to include an exponential term as

$$\begin{aligned}\hat{J} &= \frac{1}{2}e^{2\alpha t_f}\mathbf{e}'(t_f)\mathbf{F}(t_f)\mathbf{e}(t_f) \\ &+\frac{1}{2}\int_{t_0}^{t_f} e^{2\alpha t}\left[\mathbf{e}'(t)\mathbf{Q}\mathbf{e}(t)+\mathbf{u}'(t)\mathbf{R}\mathbf{u}(t)\right]dt\end{aligned} \tag{13}$$

where α is a positive parameter. We need to find the optimal control which minimizes the new performance index $\hat{J}$ (13) under the dynamical constraint (3). This problem can be solved by modifying the original system, so the following transformations can be developed as

$$\begin{aligned}&\mathbf{e}(t)=e^{\alpha t}\mathbf{e}(t); \quad \hat{\mathbf{z}}(t)=e^{\alpha t}\mathbf{z}(t);\\ &\hat{\mathbf{x}}(t)=e^{\alpha t}\mathbf{x}(t); \quad \hat{\mathbf{u}}(t)=e^{\alpha t}\mathbf{u}(t).\end{aligned} \tag{14}$$

Then, using the transformations (13), it is easy to see that the *new* system becomes

$$\begin{aligned}\dot{\hat{\mathbf{x}}}(t)=\frac{d}{dt}\{e^{\alpha t}\mathbf{x}(t)\} &= \alpha e^{\alpha t}\mathbf{x}(t)+e^{\alpha t}\dot{\mathbf{x}}(t)\\ &= \alpha\hat{\mathbf{x}}(t)+e^{\alpha t}[\mathbf{A}\mathbf{x}(t)+\mathbf{B}\mathbf{u}(t)]\\ \dot{\hat{\mathbf{x}}}(t) &= (\mathbf{A}+\alpha\mathbf{I})\hat{\mathbf{x}}(t)+\mathbf{B}\hat{\mathbf{u}}(t).\end{aligned} \tag{15}$$

Considering the minimization of the modified system defined by (15) and (13), the new optimal control $\hat{\mathbf{u}}^*(t)$, which is similar to (11), is given by

$$\hat{\mathbf{u}}^*(t)=-\mathbf{R}^{-1}\mathbf{B}'\hat{\mathbf{P}}(t)\hat{\mathbf{x}}^*(t)+\mathbf{R}^{-1}\mathbf{B}'\hat{\mathbf{g}}(t). \tag{16}$$

Here, the matrix $\hat{\mathbf{P}}(t)$ and the vector $\hat{\mathbf{g}}(t)$ are respectively the solutions of DRE

$$\begin{aligned}\dot{\hat{\mathbf{P}}}(t) &= -\hat{\mathbf{P}}(t)(\mathbf{A}+\alpha\mathbf{I})-(\mathbf{A}'+\alpha\mathbf{I})\hat{\mathbf{P}}(t)\\ &+\hat{\mathbf{P}}(t)\mathbf{B}\mathbf{R}^{-1}\mathbf{B}'\hat{\mathbf{P}}(t)-\mathbf{Q},\end{aligned} \tag{17}$$

with final condition $\hat{\mathbf{P}}(t_f)=\mathbf{F}(t_f)$, and the non-homogeneous vector differential equation

$$\dot{\hat{\mathbf{g}}}(t)=-\left[\mathbf{A}+\alpha\mathbf{I}-\mathbf{B}\mathbf{R}^{-1}\mathbf{B}'\hat{\mathbf{P}}(t)\right]'\hat{\mathbf{g}}(t)-\mathbf{Q}\hat{\mathbf{z}}(t), \tag{18}$$

with final condition $\hat{\mathbf{g}}(t_f)=\mathbf{F}(t_f)\hat{\mathbf{z}}(t_f)$. Using the optimal control (16) in the new system (15), we get the optimal closed-loop system as

$$\dot{\hat{\mathbf{x}}}^*(t)=\left[\mathbf{A}+\alpha\mathbf{I}-\mathbf{B}\mathbf{R}^{-1}\mathbf{B}'\hat{\mathbf{P}}(t)\right]\hat{\mathbf{x}}^*(t)+\mathbf{B}\mathbf{R}^{-1}\mathbf{B}'\hat{\mathbf{g}}(t) \tag{19}$$

with initial condition $\hat{\mathbf{x}}(t_0)$.

Hence, applying the transformations (15) in the new system (16), the optimal control of the original system (3) and the associated performance measure (13) is given by

$$\begin{aligned}\mathbf{u}^*(t)=e^{-\alpha t}\hat{\mathbf{u}}^*(t) &= -e^{-\alpha t}\mathbf{R}^{-1}\mathbf{B}'\left[\hat{\mathbf{P}}(t)\hat{\mathbf{x}}^*(t)-\hat{\mathbf{g}}(t)\right]\\ &= -\mathbf{R}^{-1}\mathbf{B}'\hat{\mathbf{P}}(t)\mathbf{x}^*(t)+e^{-\alpha t}\mathbf{R}^{-1}\mathbf{B}'\hat{\mathbf{g}}(t).\end{aligned} \tag{20}$$

Interestingly, this desired (original) optimal control (20) has the same matrix DRE solutions $\hat{\mathbf{P}}(t)=\mathbf{P}(t)$ as the optimal control (6) of the new system with $\hat{\mathbf{g}}(t)=e^{\alpha t}\mathbf{g}(t)$ compared with (20) and (11). We see that the closed-loop optimal control system (19) has eigenvalues with real parts less than $-\alpha$. In other words, the state $\mathbf{x}^*(t)$ approaches zero at least as fast as $e^{-\alpha t}$.

III. SIMULATION RESULTS AND DISCUSSION

We present simulations with the GA-tuned PID controller and modified linear quadratic finite-time optimal controller with tracking system for the 14-DoF, five-finger smart robotic hand in order to grasp a rectangular object. In this work, the first and second joint angles of the thumb are constrained in the ranges of [0, 90] and [-80, 0] (degrees) and the first, second, and third joint angles of the other four fingers are constrained in the ranges of [0, 90], [0, 110] and [0, 80] (degrees), respectively [14]. All parameters of the robotic hand selected for the simulations [15] are given in Table **1** and the side length and length of the targeted rectangular rod are 0.01 and 0.1 (m), respectively. The conversion parameters between the global coordinate and each local coordinate are defined in Table **2** [12, 13]. The links of all fingers are assumed as circular cylinders with the radius (R) 0.010 (m) and the inertia I_{zzk}^j of each link k of all fingers j ($=t$, i, m, r and l) can be calculated by

$$I_{zzk}^j=\frac{1}{4}m_k^jR^2+\frac{1}{3}m_k^jL_k^{j2}. \tag{21}$$

Table 1: Parameter Selection of the Robotic Hand

Parameters	Values
Thumb	
Time (t_0, t_f)*	0, 20 (sec)
Desired Initial Position (X_0^t, Y_0^t)**	0.035, 0.060 (m)
Desired Final Position (X_f^t, Y_f^t)**	0.0495, 0.060 (m)
Desired Initial Velocity $(\dot{X}_0^t, \dot{Y}_0^t)$*	0, 0 (m/s)
Desired Final Velocity $(\dot{X}_f^t, \dot{Y}_f^t)$*	0, 0 (m/s)
Length (L_1^t, L_2^t)	0.040, 0.040 (m)
Mass (m_1^t, m_2^t)	0.043, 0.031 (kg)
Index Finger	
Desired Initial Position (X_0^i, Y_0^i)**	0.065, 0.080 (m)
Desired Final Position (X_f^i, Y_f^i)**	0.010, 0.060 (m)
Length (L_1^i, L_2^i, L_3^i)	0.040, 0.040, 0.030 (m)
Mass (m_1^i, m_2^i, m_3^i)	0.045, 0.025, 0.017 (kg)
Middle Finger	
Desired Initial Position (X_0^m, Y_0^m)**	0.065, 0.080 (m)
Desired Final Position (X_f^m, Y_f^m)**	0.005, 0.060 (m)
Length (L_1^m, L_2^m, L_3^m)	0.044, 0.044, 0.033 (m)
Mass (m_1^m, m_2^m, m_3^m)	0.050, 0.028, 0.017 (kg)
Ring Finger	
Desired Initial Position (X_0^r, Y_0^r)**	0.065, 0.080 (m)
Desired Final Position (X_f^r, Y_f^r)**	0.010, 0.060 (m)
Length (L_1^r, L_2^r, L_3^r)	0.040, 0.040, 0.030 (m)
Mass (m_1^r, m_2^r, m_3^r)	0.041, 0.023, 0.014 (kg)
Little Finger	
Desired Initial Position (X_0^l, Y_0^l)**	0.055, 0.080 (m)
Desired Final Position (X_f^l, Y_f^l)**	0.020, 0.060 (m)
Length (L_1^l, L_2^l, L_3^l)	0.038, 0.038, 0.030 (m)
Mass (m_1^l, m_2^l, m_3^l)	0.041, 0.023, 0.014 (kg)

*All fingers use same parameters.
**All parameters are in local coordinates.

Table 2: Parameter Selection of Conversion Between Global and Local Coordinates

Parameters	Values
Rotating α	90 (deg)
Rotating β	45 (deg)
Translating $\mathbf{d}^i$	(0.035, 0, 0) (m)
Translating $\mathbf{d}^m$	(0.040, 0, -0.020) (m)
Translating $\mathbf{d}^r$	(0.035, 0, -0.040) (m)
Translating $\mathbf{d}^l$	(0.025, 0, -0.060) (m)

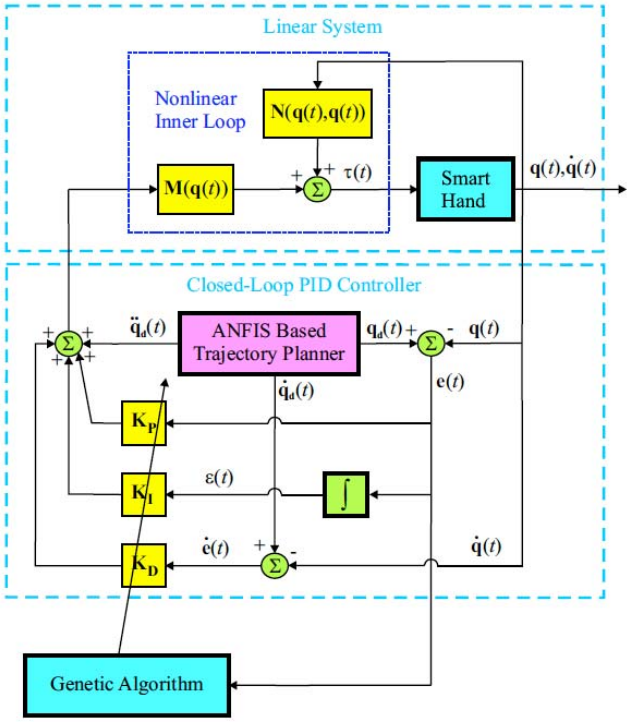

Figure 2: Block Diagram of the Hybrid GA-Based PID Controller for the 14-DoF, Five-Finger Robotic Hand.

All initial actual angles are zero. Figure **2** shows the block diagram of a hybrid GA-based PID controller. From the derived dynamic and control models, after the parameters ($\mathbf{K_P}$, $\mathbf{K_I}$ and $\mathbf{K_D}$) are determined, the torque matrix $\boldsymbol{\tau}$ can be calculated, and then the squared-tracking errors $e_i^j(t)$ of the joint i of the finger j are obtained. Thus, the total error $E(t)$, a time-dependent function, can be defined as

$$E(t) = \int_{t_0}^{t_f} (e_i^j(t))^2 dt, \tag{22}$$

where t_0 and t_f are initial and terminal time, respectively. The tuned diagonal parameters ($\mathbf{K_P}$, $\mathbf{K_I}$

Table 3: Parameter Selection of GA-Tuned PID Controller and Computed Total Errors

	Input			Output
Fingers	**K_P**	**K_I**	**K_D**	*E(t)*
Thumb	[976,956]	[779,279]	[170,236]	0.3107
Index	[794,398,960]	[960,918,914]	[15,59,242]	0.0465
Middle	[794,398,960]	[960,918,914]	[15,59,242]	0.1003
Ring	[794,398,960]	[960,918,914]	[15,59,242]	0.0465
Little	[794,398,960]	[960,918,914]	[15,59,242]	0.0607

and $\mathbf{K_D}$) and the total error $E(t)$ of PID controller by GA are listed in Table **3** based on our previous study [2]. As for the coefficients of optimal control, $\mathbf{A}$, $\mathbf{B}$, $\mathbf{F}(t_f)$, $\mathbf{R}$ and $\mathbf{Q}$ of all fingers (j = i, m, r, and l) are chosen as

$$\mathbf{A}=\begin{bmatrix}\mathbf{0} & \mathbf{I}\\ \mathbf{0} & \mathbf{0}\end{bmatrix},\ \mathbf{B}=\begin{bmatrix}\mathbf{0}\\ \mathbf{I}\end{bmatrix},\ \mathbf{F}(t_f)=\mathbf{0},\ \mathbf{R}=\frac{1}{30}\mathbf{I},$$

$$\mathbf{Q}^t=\begin{bmatrix}\mathbf{Q_{11}} & \mathbf{Q_{12}}\\ \mathbf{Q_{12}'} & \mathbf{Q_{22}}\end{bmatrix},\ \mathbf{Q}^j=\begin{bmatrix}\mathbf{Q_{11}} & \mathbf{Q_{12}} & \mathbf{Q_{13}}\\ \mathbf{Q_{12}'} & \mathbf{Q_{22}} & \mathbf{Q_{23}}\\ \mathbf{Q_{13}'} & \mathbf{Q_{23}'} & \mathbf{Q_{33}}\end{bmatrix},$$

$$\mathbf{Q_{11}}=\begin{bmatrix}10 & 2\\ 2 & 10\end{bmatrix},\ \mathbf{Q_{22}}=\begin{bmatrix}30 & 0\\ 0 & 30\end{bmatrix},\ \mathbf{Q_{33}}=\begin{bmatrix}20 & 1\\ 1 & 20\end{bmatrix},$$
$$\mathbf{Q_{12}}=\begin{bmatrix}-4 & 4\\ 3 & -6\end{bmatrix},\mathbf{Q_{13}}=\begin{bmatrix}-4 & 4\\ 3 & -6\end{bmatrix},\mathbf{Q_{23}}=\begin{bmatrix}-4 & 3\\ 4 & -6\end{bmatrix}.$$

To compare the performance of the GA-tuned PID and modified optimal controllers, Figures **3**, **4** show desired/actual angles and tracking errors of joints 1 and 2 for two-link thumb, respectively. GA-tuned PID control shows an overshooting problem. The problem is overcome by the original optimal control (α = 0), but it takes at least 10 seconds for both joints. The performance is improved by the proposed optimal controller as the parameter α increases from 1 to 10. In other words, the convergence time is reduced to approximate 0.2 second as α is 10. For three-link index finger, the GA-tuned PID control causes not only overshooting but also oscillation problems as shown in Figures **5a**, **6a**. The optimal control with modified performance index ($\hat{J}$) embedded with an exponential term (α) also overcomes the overshooting and oscillation problems and obtains faster convergence speed as α increases. Similar simulations are also made for other three-link fingers. Taken together, these data suggest that the modified optimal control has higher accuracy and faster convergence speed than GA-tuned PID control.

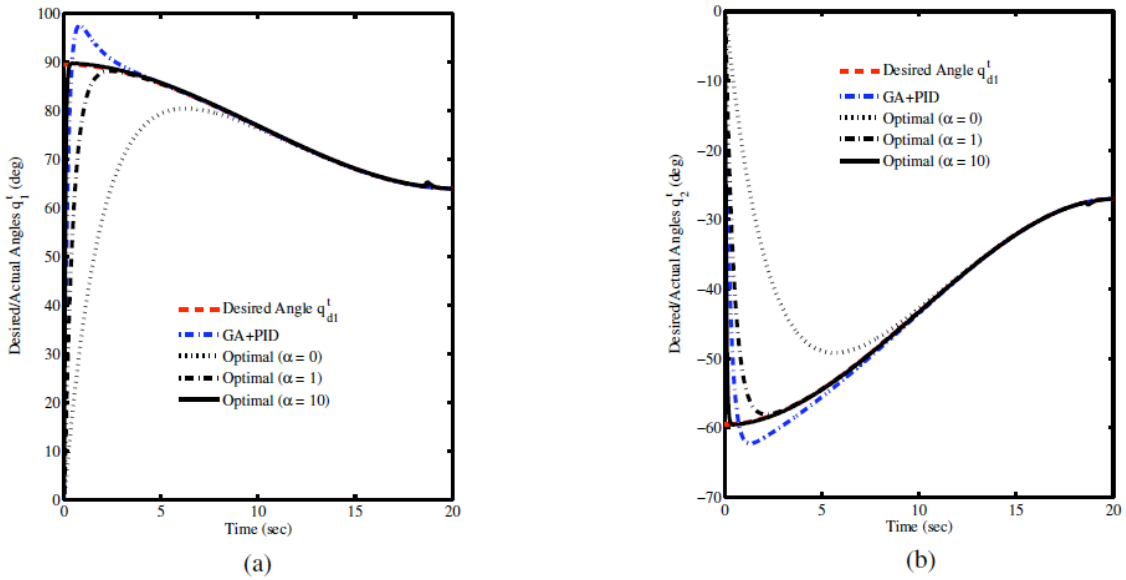

Figure 3: Desired/actual angular positions of two-link thumb: the actual angles (**a**) q_1^t and (**b**) q_2^t regulated by GA-tuned PID controller (blue line) and modified optimal controller (black lines) with the different parameters α (α = 0, 1, and 10) are designed to track the desired angles q_{d1}^t and q_{d2}^t (red line).

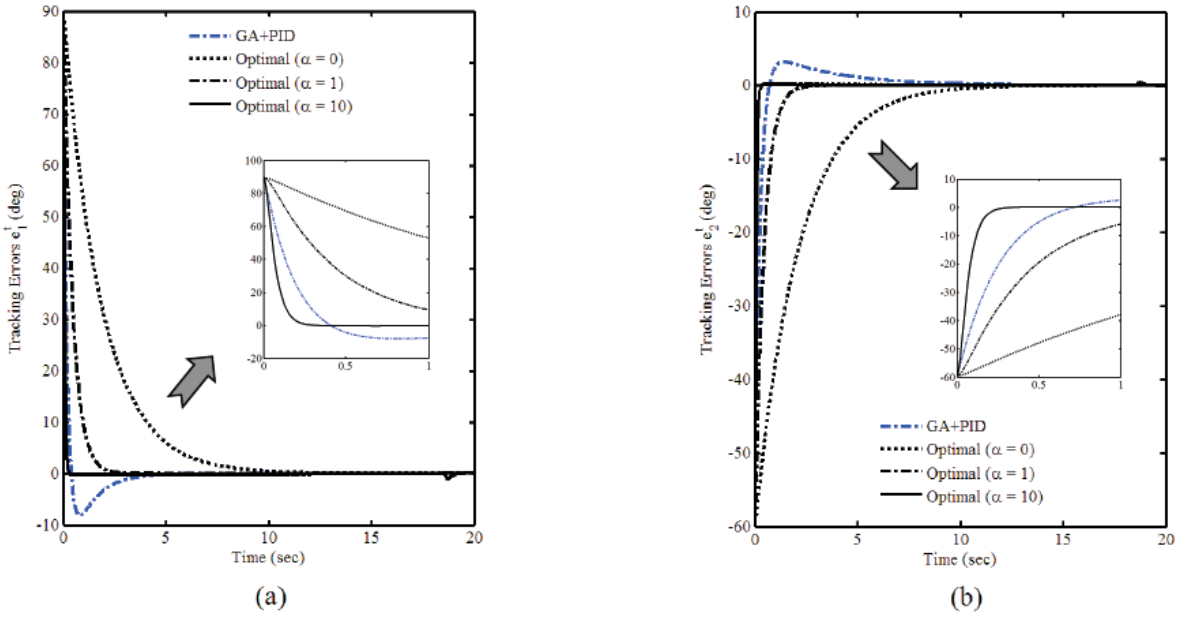

Figure 4: Tracking errors of two-link thumb: the tracking errors (**a**) e_1^t and (**b**) e_2^t show that PID controller with GA-tuned parameters (blue line) has an overshooting problem, which is overcome by the proposed modified optimal controller with α = 0, 1, and 10.

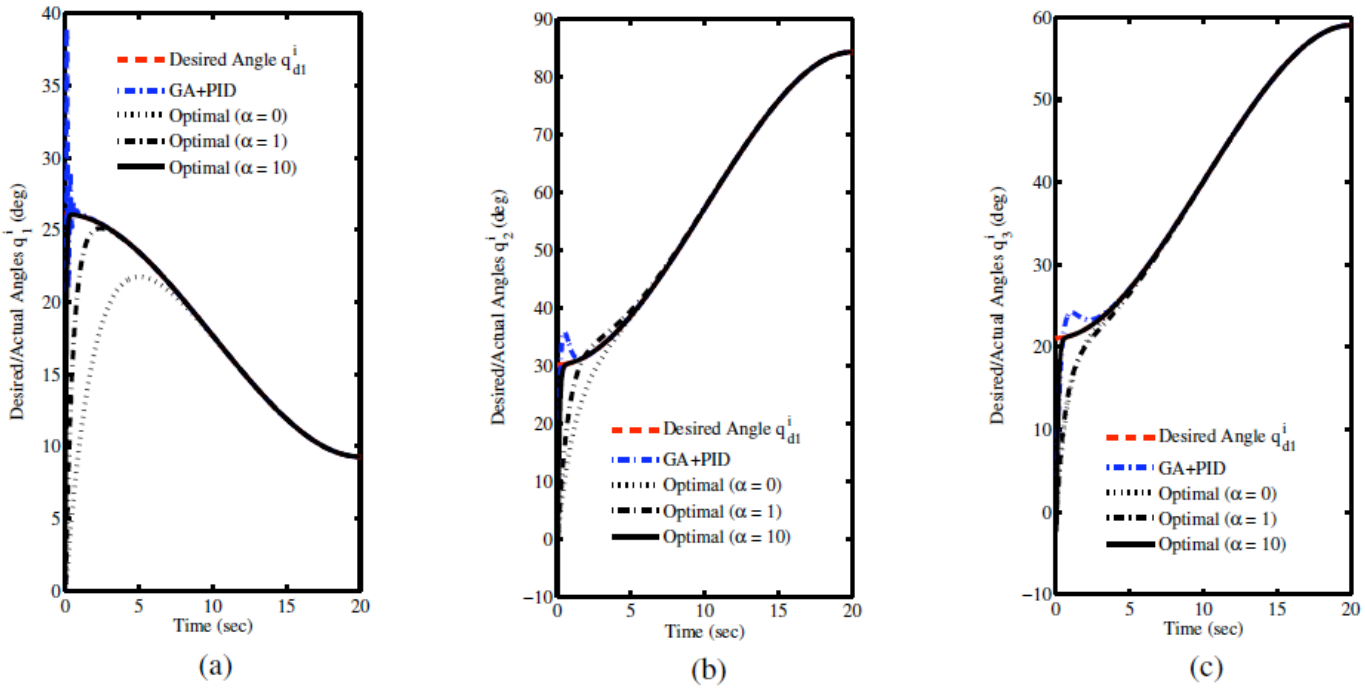

Figure 5: Desired/actual angular positions of three-link index finger: the actual angles (**a**) q_1^i, (**b**) q_2^i and (**c**) q_3^i regulated by GA-tuned PID controller and proposed optimal controller with the different parameters α (α = 0, 1, and 10) are designed to track the desired angles q_{d1}^i, q_{d2}^i and q_{d3}^i, respectively.

We then ask the question whether the modified optimal control has less computational time than GA-based PID control. To investigate the effectiveness of the GA-based PID and modified optimal controllers, Figure **7** shows that original (α = 0) and new optimal controllers (α = 0.1, 1, and 10) are significantly more effective (in term of computational time) than GA-PID controller, but there is no significance between the

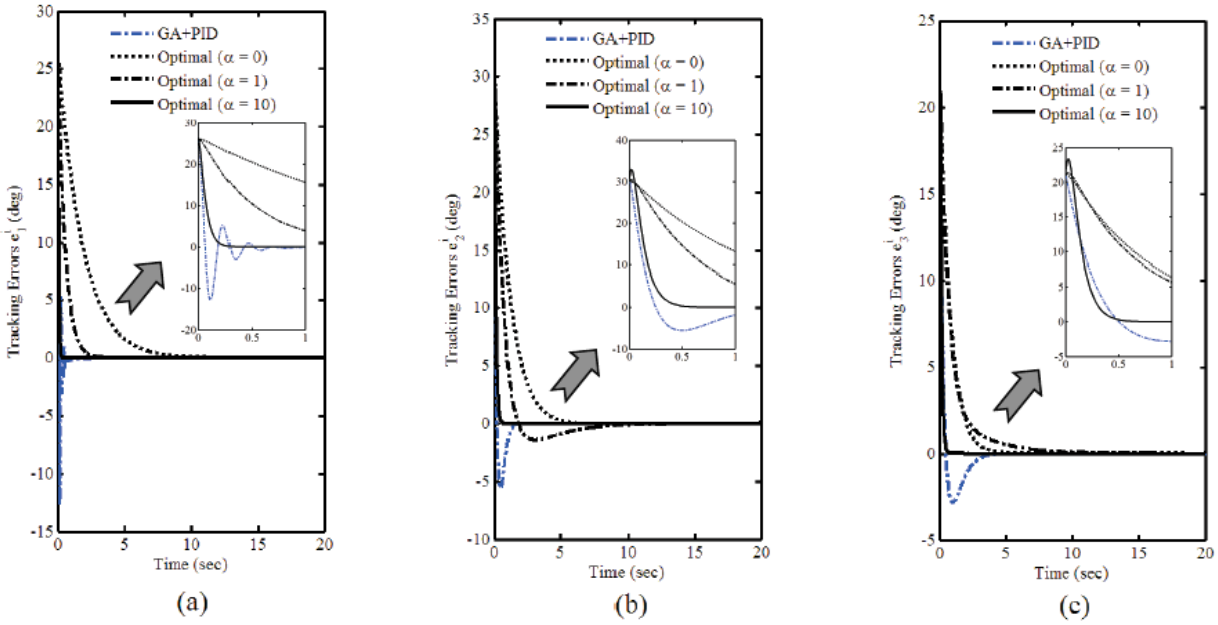

Figure 6: Tracking errors of three-link index finger: the tracking errors (**a**) e_1^i, (**b**) e_2^i and (**c**) e_3^i show that the modified optimal controller acts faster than GA-based PID controller as the parameter α increases from 0 to 10.

optimal controllers for all three-link fingers, suggesting that the new optimal control with high α value improves performance without excessive execution time. The simulations were simulated by a laptop with Intel © Core2 Duo CPU at 1.67 GHz.

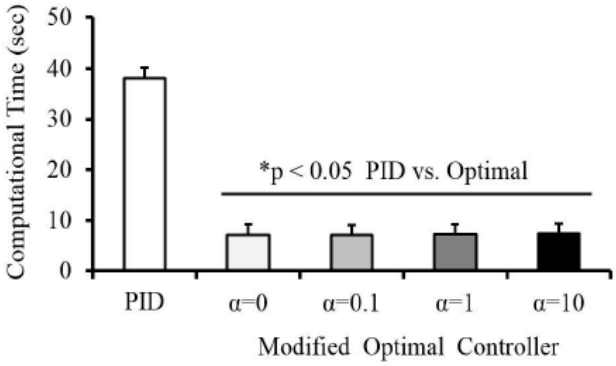

Figure 7: The modified optimal controller significantly reduces execution time (*p < 0.05, vs. GA-tuned PID control, n=8).

IV. CONCLUSIONS AND FUTURE WORK

A modified optimal control strategy for a 14-DoF, five-finger smart robotic hand was successfully developed to improve performance, convergence speed and computational time compared to a hybrid GA-based PID control. This modified technique can be tested and validated with robotic applications, including operation of prosthetic hand devices with real data from surface electromyographic (sEMG) signals.

ACKNOWLEDGMENT

The research was sponsored by the U.S. Department of the Army, under the award number W81XWH-10-1-0128 awarded and administered by the U.S. Army Medical Research Acquisition Activity, 820 Chandler Street, Fort Detrick, MD 21702-5014, USA. The information does not necessarily reflect the position or the policy of the Government, and no official endorsement should be inferred. For purposes of this article, information includes news releases, articles, manuscripts, brochures, advertisements, still and motion pictures, speeches, trade association proceedings, etc. We appreciate the reviewers' comments improving this work.

REFERENCES

[1] Chen C-H, Naidu DS, Perez-Gracia A, Schoen MP. A hybrid control strategy for five-fingered smart prosthetic hand, in Joint 48th IEEE Conference on Decision and Control (CDC) and 28th Chinese Control Conference (CCC), Shanghai, P. R. China, December 16-18 2009; pp. 5102-5107.

[2] Chen C-H, Naidu DS. Hybrid genetic algorithm PID control for a five-fingered smart prosthetic hand, in Proceedings of the 6th International Conference on Circuits, Systems and Signals (CSS'11), Vouliagmeni Beach, Athens, Greece, March 7-9 2012; pp. 57-63.

[3] Subudhi B, Morris AS. Soft computing methods applied to the control of a flexible robot manipulator. Applied Soft Computing 2009; 9: 149-158. http://dx.doi.org/10.1016/j.asoc.2008.02.004

[4] Liu F, Chen H. Motion control of intelligent underwater robot based on CMAC-PID, in Proceedings of the 2008 IEEE

International Conference on Information and Automation, Zhangjiajie, China, June 20-23 2008; pp. 1308-1311.

[5] Naidu D. Optimal Control Systems. Boca Raton, FL: CRC Press 2003.

[6] Chen C-H, Naidu DS, Perez-Gracia A, Schoen MP. A hybrid optimal control strategy for a smart prosthetic hand, in Proceedings of the ASME 2009 Dynamic Systems and Control Conference (DSCC), Hollywood, California, USA, October 12-14 2009; (No. DSCC2009-2507).

[7] Kim K, Colgate JE. Haptic feedback enhances grip force control of sEMG-controlled prosthetic hands in targeted reinnervation amputees. IEEE Transactions on Neural Systems and Rehabilitation Engineering 2012; 20(6): 798-805. http://dx.doi.org/10.1109/TNSRE.2012.2206080

[8] Kamavuako EN, Rosenvang JC, Bøg MF, Smidstrup A, Erkocevic E, Niemeier MJ, Jensen W, Farina D. Influence of the feature space on the estimation of hand grasping force from intramuscular EMG. Biomedical Signal Processing and Control 2013; 8: 1-5. http://dx.doi.org/10.1016/j.bspc.2012.05.002

[9] Engeberg ED. A physiological basis for control of a prosthetic hand. Biomedical Signal Processing and Control 2013; 8: 6-15. http://dx.doi.org/10.1016/j.bspc.2012.06.003

[10] Naidu DS, Chen C-H, Perez A, Schoen MP. Control strategies for smart prosthetic hand technology: An overview, in The 30th Annual International Conference of the IEEE Engineering Medicine and Biology Society (EMBS), Vancouver, Canada, August 20-24 2008; pp. 4314-4317.

[11] Naidu DS, Chen C-H. Automatic Control Techniques for Smart Prosthetic Hand Technology: An Overview, book chapter 12, to appear in a book titled "Distributed Diagnosis and Home Healthcare (D_2H_2): Volume 2". California, USA: American Scientific Publishers 2011.

[12] Chen C-H, Naidu DS, Schoen MP. Adaptive control for a five-fingered prosthetic hand with unknown mass and inertia. World Scientific and Engineering Academy and Society (WSEAS) Journal on Systems 2011; 10(5): 148-161.

[13] Chen C-H, Naidu DS. Hybrid control strategies for a five-finger robotic hand. Biomedical Signal Processing and Control 2013; 8(4): 382-390. http://dx.doi.org/10.1016/j.bspc.2013.02.003

[14] Lavangie PK, Norkin CC. Joint Structure and Function: A Comprehensive Analysis, Third Edition. Philadelphia, PA: F. A. Davis Company 2001.

[15] Arimoto S. Control Theory of Multi-fingered Hands: A Modeling and Analytical-Mechanics Approach for Dexterity and Intelligence. London, UK: Springer-Verlag 2008.

Received on 23-06-2014 Accepted on 16-07-2014 Published on 18-11-2014